Canadian Conference - Pacific Conference on Earthquake Engineering 2023
Vancouver, British Columbia
June 25th – June 30th, 2023

Large-Scale Seismic Simulation for Site-City Interaction Analysis

Mohamed A. Sayed[1] and Oh-Sung Kwon[2*]

[1]PhD Candidate, Department of Civil and Mineral Engineering, University of Toronto, Toronto, Ontario, Canada
[2]Professor, Department of Civil and Mineral Engineering, University of Toronto, Toronto, Ontario, Canada
[*]os.kwon@utoronto.ca (Corresponding Author)

ABSTRACT

Conventional seismic design of a building in a dense urban area typically ignores the effect of nearby buildings on ground motion while imposing undisturbed free-field motion at the base of the building. Therefore, it is necessary to develop a detailed site-city model to capture the dynamic interaction between the site and buildings in a city during an earthquake. The challenges of creating detailed site-city models include capturing the site's complex geometric and material heterogeneity, such as surface and bedrock topography and soil lithology. In addition, modelling a large inventory of buildings incorporating their geometry, location, and mechanical properties to simulate their dynamic response remains challenging. This study presents the development of a framework for creating, analyzing, and post-processing large-scale site-city models considering site-city interaction. The created models incorporate the actual geometry of buildings from 2D layouts or 3D massing models, while the geometric and material heterogeneity of soil strata is created from borehole logs. Dynamic analysis is conducted on a supercomputer cluster. An investigation is conducted of a city block composed of 23 buildings in a site modelled using 327 borehole logs. There are two approaches to modelling buildings: idealized geometry and actual geometry. The results show that the presence of buildings reduces the surface ground motion within the city block and that the idealized geometry of buildings underestimates their dynamic response compared to actual geometry, especially for buildings with high in-plane and vertical geometric irregularities.

Keywords: site-city interaction, large-scale simulation, city block, supercomputer

INTRODUCTION

The growth of the world economy has resulted in the emergence of urban areas with high population densities and complex infrastructures. The physical proximity between buildings, underground spaces, and subway stations is often a defining feature of urban areas. However, in the seismic hazard studies of buildings in such areas, the impact of buildings on ground motion is often overlooked. Instead, undisturbed free-field motion at the base of buildings is assumed [1,2]. In addition, numerous studies have highlighted the importance of accounting for soil-structure interaction (SSI) in seismic analyses. For example, Bard et al. [3] and Chavez-Garcia and Cardenas-Soto [4] have advised that free-field ground motions in densely urbanized sites should be treated carefully due to the potential impact of structure-soil-structure interaction.

Various factors influence how a site responds to an earthquake, including the local site effect, which results from the properties of soil layers and site characteristics, such as subsurface soil heterogeneity and surface topography [5]. In urban areas, the presence of adjacent buildings often leads to multiple SSIs, which can affect the seismic response of a building. Wong and Trifunac [6] observed that the arrangement of buildings within a group could impact their seismic response, especially if heavier and larger structures surround the building of interest. Moreover, the waves trapped between the embedded foundations of buildings due to multiple SSIs can cause disruptions in the foundations of nearby buildings. Several earthquakes, such as the 1906 earthquake in San Francisco, the 1985 earthquake in Mexico, and the 1995 earthquake in Kobe, Japan [1], have demonstrated that site conditions are a significant factor in earthquake damage. However, site-city interaction (SCI) only gained significant attention after the 1985 earthquake in Mexico City, which revealed that the built environment could cause considerably larger amplifications and long-duration surface motions than free-field motions without buildings [1,2].

Previous research (e.g., Bard et al. [3]; Taborda and Bielak [7]; Schwan et al. [8]) have investigated SCI analytically, numerically, and experimentally, but with simplifications in modelling the site and buildings. However, accurately capturing the SCI effect on the ground and buildings' responses requires a detailed model that considers many parameters, such as the actual arrangement and geometry of buildings, their mechanical properties, and the site's topographic and geological features and material heterogeneity. Furthermore, creating large-scale site models with high fidelity necessitates detailed borehole or GIS data. Previous studies (e.g., Taborda and Bielak [7]; Isbiliroglu et al. [9]; Sayed et al. [10]; Kato and Wang [11]) have developed sophisticated site-city models to investigate the SCI effect. However, they often neglected one or more of the parameters that influence SCI due to the inherent complexity of the problem. As a result, there is still a lack of comprehensive models that can accurately capture the SCI effect.

This study presents the development of an SCI framework for semi-automatically generating detailed 3D site-city models that can overcome the current shortcomings in modelling detailed site-city models. The framework enables the modelling of geometric features and the heterogeneity of soil strata from borehole logs, which allows the seismic response analysis to consider surface and bedrock topography effects. It also allows the modelling of buildings' actual arrangement and geometry in the region of interest. The framework employs high-performance computing (HPC) to analyze and visualize results.

The paper is organized in the following manner. The first section is an introduction, followed by a detailed description of the SCI framework and an overview of the development of the site-city model components. Subsequently, the analysis and post-processing procedures of the models are outlined. Then, an application of the framework to a city block in downtown Toronto is presented. Finally, the paper concludes with a summary of the results and conclusions.

SITE-CITY INTERACTION FRAMEWORK

Figure 1 depicts a schematic representation of the modelling and analysis of a site-city model in the framework. The model consists of two main components: the site and the buildings. Creating an accurate model requires the creation of actual geometry and assigning appropriate material properties to the components to accurately capture their dynamic responses during seismic wave propagation. First, a three-dimensional (3D) soil model is created in a few steps using existing borehole logs in the region of interest. The borehole data is first processed by filtering and reading the soil layer description. Subsequently, soil properties required for conducting linear elastic analysis, such as shear wave velocity, mass density, and Poisson's ratio, are assigned and correlated to the extracted soil layer description. Using RockWorks [12], the geometry of the soil model is then generated through interpolation and extrapolation of borehole logs. Finally, the surface and bedrock topography of the site is created in the soil model by incorporating information from the borehole logs.

Modelling the geometry of buildings is primarily based on information extracted from the available two-dimensional (2D) layout or 3D massing model of the region of interest. The information involves the location, height, and footprint of buildings. The information is then utilized to create the geometry of the superstructure of buildings, which is represented as 3D homogeneous blocks. However, details such as the number of storeys, storey height, and depth of basements are still unavailable but needed in creating the geometry of buildings, which are assumed in the modelling process. Also, the material properties for the superstructure and basement portions are still needed to reproduce buildings' modal and dynamic responses. After the site-city model is discretized, system matrices are extracted for dynamic analysis and visualization on a supercomputer cluster. Additional information regarding creating and analyzing the site-city model is discussed in the following section.

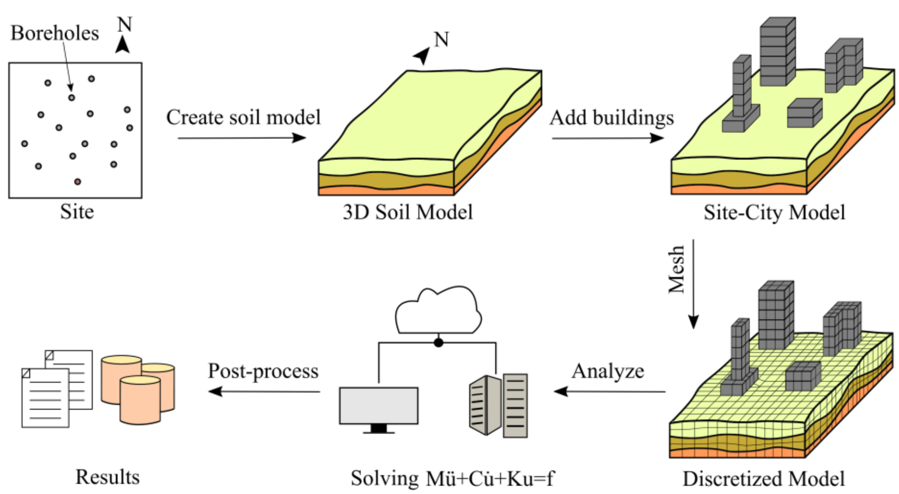

Figure 1. Schematic representation of the framework.

SITE-CITY MODELLING

Creating a site-city model involves several steps, such as generating the site model, incorporating the geometry of buildings, integrating the site and city models, and ultimately discretizing the model. The various steps involved in this procedure are explained in the following subsections.

Site Modelling

The dimensions of the soil model are specified in terms of length, width, and depth, ensuring adequate coverage of the region of interest. The model is then divided into uniform 3D grids. The available borehole logs are then utilized to develop the soil model. Therefore, the lateral extrusion algorithm is employed to interpolate and extrapolate borehole data, extruding the soil layer in every borehole horizontally to the midpoint between the adjacent borehole log, preventing the creation of random soil layers between boreholes. The ground surface level data obtained from each borehole is also used to construct the site's surface topography. The grids are subsequently populated with soil layers. All the above steps are performed in RockWorks.

The material properties of soil layers are required to conduct dynamic analysis. The data extracted from borehole logs are used to assign the various material properties of soil layers. First, the parsed descriptive keywords of soil layers in the borehole logs are correlated with the field standard penetration test (SPT) N-value. For instance, keywords such as loose, compact, or dense are linked with the density of cohesionless soil layers, whereas keywords such as soft, firm, stiff, or hard are connected with the consistency of cohesive soil layers. A set of N-values is then selected corresponding to the parsed keywords. Subsequently, the shear wave velocity is estimated using the N-value through the following equation:

$$V_s = \mathrm{a}N^b \tag{1}$$

where, V_s is shear wave velocity, a and b are constants that depend on the soil type, whether cohesionless or cohesive soil. For example, Hasancebi and Ulusay [13] proposed a and b values of 90.82 and 0.319 for cohesionless soil and 97.89 and 0.269 for cohesive soil. Similarly, mass density and Poisson's ratio of soil layers are estimated corresponding to the descriptive keywords. The determined material properties are then allocated to the respective soil layers for model discretization and analysis.

City Modelling

Modelling buildings starts with reading the available 2D layouts or 3D massing models that contain information such as the actual location, shape, and total height of the buildings. Such a procedure enables modelling a vast inventory of buildings, even when detailed drawings are unavailable. Fortunately, many websites offer free access to massing models for cities worldwide. The next step involves modelling buildings' superstructure and basement blocks as 3D homogeneous blocks that reproduce the layout and shape of buildings, as shown in Figure 2. The shape of the basement block is assumed to mimic the outer perimeter of the superstructure block.

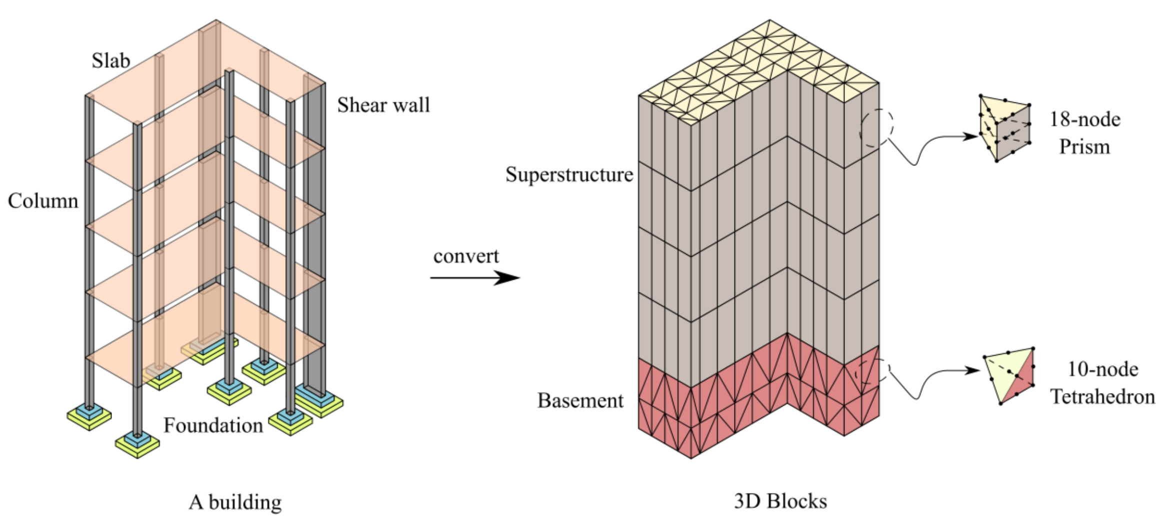

Figure 2. Modelling and mesh discretization of buildings.

The material properties of the superstructure block of a building are assigned to replicate its dynamic characteristics without information about its lateral load-resisting systems. First, the mass density is assigned as 300 kg/m^3 following previous studies (e.g., Taborda and Bielak [7]; Isbiliroglu et al. [9]; Kato and Wang [14]). The shear wave velocity is then calculated, assuming a fixed-base cantilever block, based on the building height and its estimated fundamental period, following previous studies (e.g., Taborda [5]; Taborda and Bielak [7]; Kato and Wang [14]). However, the challenge lies in accurately estimating the fundamental period of buildings with irregular shapes based only on their height. For example, the shear wave velocity of 100 m/s estimated by Taborda and Bielak [7] overestimates the period of buildings compared to various empirical period formulas from design codes with various lateral-resisting systems. This discrepancy is because their calculations only apply to buildings with up to 12 storeys and cannot be generalized. Therefore, this study uses available building data from Toronto to calibrate the shear wave velocity. A value of 155 m/s is chosen, resulting in a fundamental period of fixed-base blocks that aligns with empirical period formulas. For more information about the procedure, refer to Sayed [15].

The depth and material properties of the basement block are needed. However, the information extracted from massing models does not include the basement or foundation depth. In such cases, the basement depth can be estimated based on generic information available for all buildings, such as their height. Furthermore, the previously mentioned building data contain information about basement depth and building height. Therefore, a relationship between building height and basement depth is established. For example, buildings between 31 and 50 m in height would have a basement depth of 6 m, while those between 51 and 100 m would have a basement depth of 9 m. As for the material properties, a mass density of 300 kg/m^3 and a shear wave velocity of 750 m/s are assumed for the basement blocks, following Isbiliroglu et al. [9].

Site-City Model

Gmsh [16] is utilized to create the model's geometry, which comprises both the site and buildings. The site and city models are merged before meshing using boolean operations in Gmsh. The soil and basement blocks are discretized into quadratic tetrahedral (10-node) elements, while the superstructure blocks are meshed into quadratic prism (18-node) elements, as illustrated in Figure 2. Quadratic prism elements are suitable for accurately capturing the complex prismatic shapes of superstructures. A characteristic length is assigned in Gmsh using Eq. 2. to determine the maximum element size for each model component.

$$l_c = \frac{V_s/f_{max}}{n} \tag{2}$$

where, l_c is the characteristic length, V_s is the shear wave velocity, n is the number of finite elements per seismic wavelength, and f_{max} is the maximum frequency desired to be resolved in the domain for seismic wave propagation. The global stiffness, mass, and viscous damping matrices are extracted from the discretized model in one analysis step employing Abaqus [17] after imposing boundary conditions. However, Abaqus is not used in the dynamic analysis due to the computational time required for a large-scale site-city model. The geometry of the site-city model is created in ParaView [18] file format to visualize the results after conducting dynamic analysis on a supercomputer cluster. ParaView is an open-source visualization application and is well-suited for visualizing large datasets.

The previous steps are carried out through a MATLAB [19] script. Initially, the script reads the soil grids filled with soil layers from RockWorks. Then it reads the information related to the buildings' 2D layout or 3D massing models and creates geometries in Gmsh format. Next, it proceeds to discretize the model. Subsequently, the script reads the mesh file and transforms it into ParaView format before converting it into an Abaqus format to generate the system matrices.

ANALYSIS AND POST-PROCESSING

The linear dynamic analysis is conducted by solving the dynamic equation of motion of the sparse system matrices using the Newmark–β method with a trapezoidal rule (γ=0.5, β=0.25). Solving for the acceleration and velocity vectors, $\ddot{\mathbf{u}}_\mathrm{t}$ and $\dot{\mathbf{u}}_\mathrm{t}$, respectively in terms of the displacement vector, $\mathbf{u}_\mathrm{t}$, under the external dynamic load vector, $\mathbf{F}$, is defined as follows:

$$\left(\frac{4}{\Delta t^2}\mathbf{M} + \frac{2}{\Delta t}\mathbf{C} + \mathbf{K}\right)\mathbf{u}_{t+\Delta t} = \mathbf{F}_{t+\Delta t} + \mathbf{M}\left(\frac{4}{\Delta t^2}\mathbf{u}_t + \frac{4}{\Delta t}\dot{\mathbf{u}}_t + \ddot{\mathbf{u}}_t\right) + \mathbf{C}\left(\frac{2}{\Delta t}\mathbf{u}_t + \dot{\mathbf{u}}_t\right) \tag{3}$$

where,

$$\begin{cases} \dot{\mathbf{u}}_{t+\Delta t} = \frac{2}{\Delta t}\left(\mathbf{u}_{t+\Delta t} - \mathbf{u}_t\right) - \dot{\mathbf{u}}_t \\ \ddot{\mathbf{u}}_{t+\Delta t} = \frac{4}{\Delta t^2}\left(\mathbf{u}_{t+\Delta t} - \mathbf{u}_t\right) - \frac{4}{\Delta t}\dot{\mathbf{u}}_t - \ddot{\mathbf{u}}_t \end{cases} \tag{4}$$

where, Δt is the time increment, $\mathbf{M}$, $\mathbf{K}$, and $\mathbf{C}$ are the mass, stiffness, and damping matrices. The dynamic analysis is carried out using the message parallel interface (MPI) for parallel computing using the Belos package [20] in the Trilinos software project [21] compiled on the Niagara supercomputer [22]. The Belos package provides a suite of iterative linear solvers suitable for large sparse linear systems. The analysis output file is in Hierarchical Data Format (HDF) format.

APPLICATION EXAMPLE

A pilot study is presented to show an application of the framework. The region of interest is located in downtown Toronto. The soil model is 2,000 m × 2,000 m, and 327 borehole logs are used to generate the soil model. The topographic map and location of borehole logs in the region of interest are shown in Figure 3(a). The highest ground surface elevation is 198 m in the top left corner, and the lowest elevation is 174 m in the bottom right corner of the soil model. The site comprises seven soil layers atop a shale bedrock. The shear wave velocity of soil layers ranges between 110 m/s for fill and 310 m/s for dense sand soil. The shear wave velocity of the shale bedrock is 800 m/s.

The city block consists of 23 buildings, covering an area of 450 m × 290 m atop the center of the soil model. Two modelling approaches are investigated to model the buildings. The first approach is the actual geometry approach which uses the real geometry and shape of buildings from the information collected from buildings layout or massing models. The second approach is the idealized approach which assumes a rectangular cuboid for a building that captures its footprint area and height. The idealized geometry ignores buildings' horizontal and vertical irregularity compared to the actual geometry. The shapes of buildings using the two approaches are illustrated in Figure 3(b). The shortest building has a height of 29 m with a fixed-base period of 0.76 s, and the tallest building has a height of 260 m with a fixed-base period of 5.2 s.

Three models have been generated for analysis. The first model (Model A) corresponds to the free-field site response analysis without buildings. The second model (Model B) represents the site-city model with idealized geometry for the buildings, and the third model (Model C) is based on the actual geometry of the buildings in the site-city model. Table 1 shows the details of the models, including the model description, number of nodes, elements, and degree-of-freedom (DOF) within each model.

All models are analyzed assuming a compliant base by applying viscous dashpots attached to the model base to emulate an elastic half-space underneath the truncated bedrock. The input motion of a Ricker wavelet is applied as an equivalent force time history in the X-direction at the model base. The translational DOFs in the Y- and Z- directions are fixed at the model base. Figure 4 shows the acceleration time history and Fourier amplitude of the Ricker input motion.

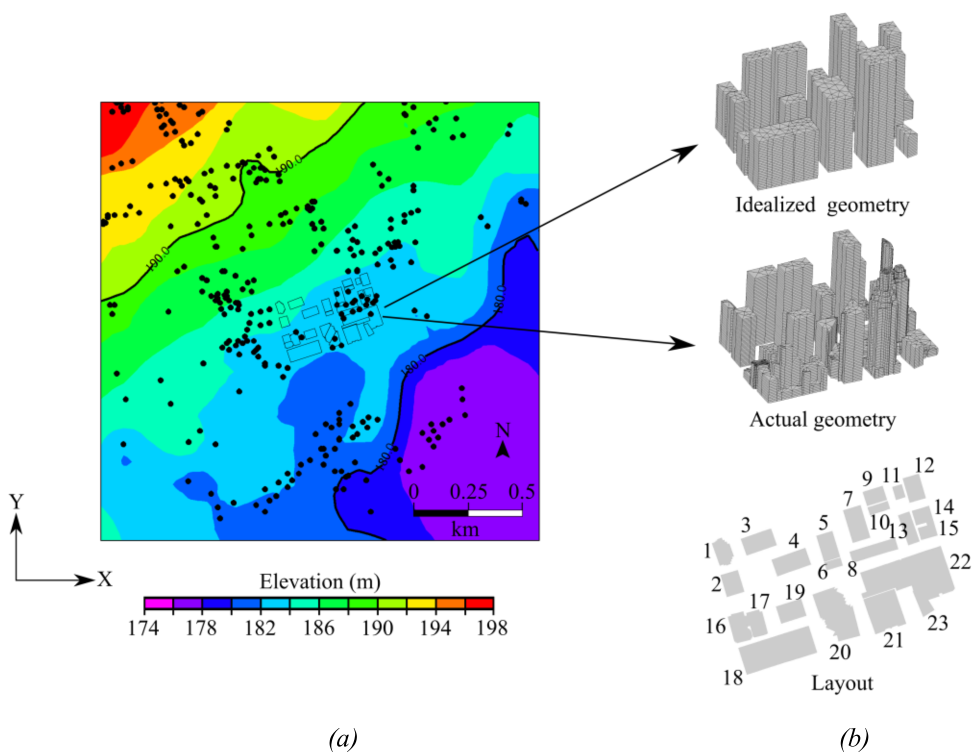

Figure 3. Region of interest: (a) topographic map and boreholes of the site, (b) geometry of buildings in the city block.

Table 1. Models details

Model	Type	Nodes	Elements	DOFs
A	Free-field	1,575,730	1,096,713	4,727,190
B	SCI w/ idealized city block	1,639,251	1,103,713	4,825,512
C	SCI w/ actual city block	1,875,281	1,185,329	5,262,588

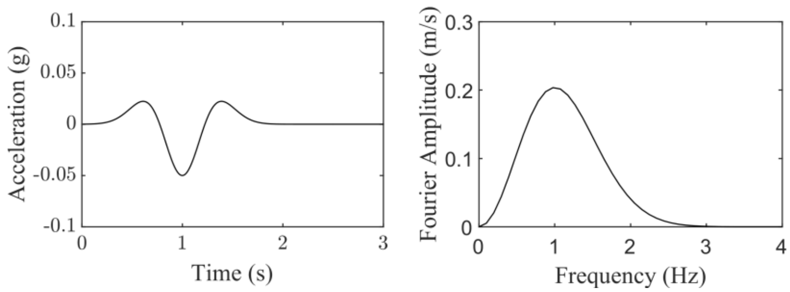

Figure 4. Acceleration time history and Fourier amplitude of the Ricker wavelet input motion.

RESULTS

The SCI effect is examined in terms of site and city responses. The site response scrutinizes the effect of SCI on the surface ground responses within and outside the city block compared to the free-field response. On the other hand, the city response evaluates the dynamic response of buildings due to SCI.

Site Response

The horizontal peak magnitude acceleration at the ground surface of the free-field model (Model A) is discussed to evaluate the site response with no buildings. The horizontal peak magnitude acceleration is calculated as the square root of the sum of the squares of the horizontal surface ground acceleration in the X- and Y-direction. The acceleration component in the X-direction primarily dominates the peak magnitude acceleration since the input motion is applied in the X-direction at the model base. However, results are plotted in favour of the peak magnitude acceleration to visualize the resultant in-plane distribution of the site response and later modifications due to SCI. The distribution of the peak magnitude acceleration at the ground surface of the free-field model is plotted in Figure 5(a). The recorded peak magnitude PGA is 0.94 m/s^2 at the city block center. The layout of the city block is only for indicating buildings' locations.

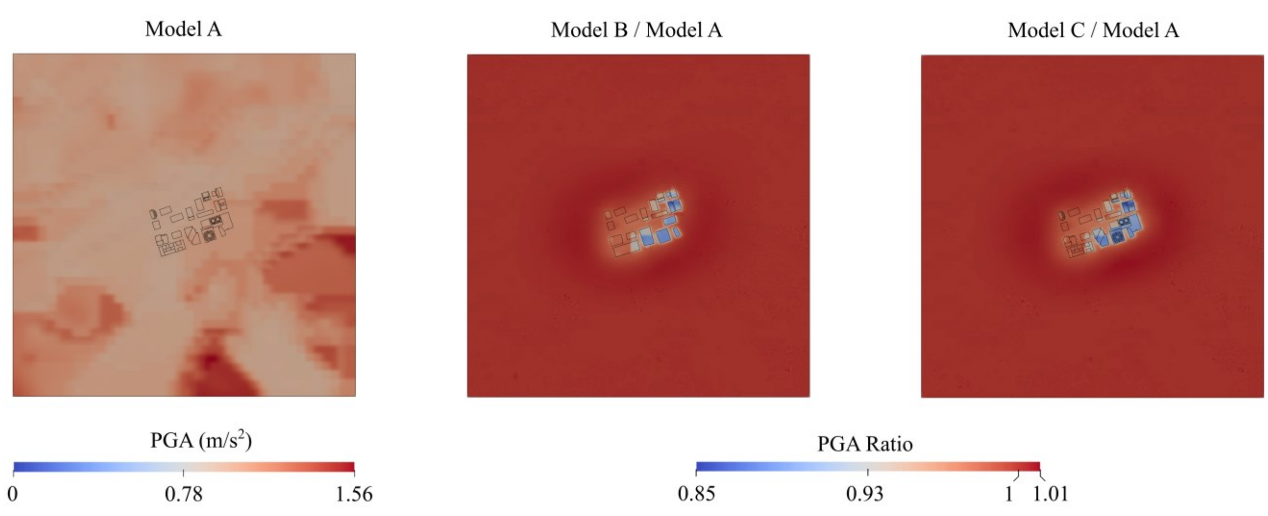

(a) *(b)*

Figure 5. Peak magnitude acceleration at the ground surface: (a) free-field model, (b) reduction due to idealized and actual site-city models.

The SCI effect is examined by investigating the changes in the free-field site response after modelling the idealized and actual city blocks. The changes are visually represented as the free-field peak magnitude acceleration reduction. The reduction factor is calculated by dividing the peak magnitude acceleration of the site-city model by that of the free-field model. When the reduction factor is lesser than one, the free-field response is de-amplified, while the free-field response is amplified when the factor is higher than one. A comparison of the reduction in peak magnitude acceleration between the idealized site-city and free-field models (Model B / Model A) and the actual site-city and free-field models (Model C / Model A) is presented in Figure 5(b). The recorded maximum reduction of the peak magnitude acceleration is 15%. Most reduction occurs at and around the buildings' locations. In addition, the reduction is primarily concentrated on the right side of the city block. Because in the free-field model, superficial soft soil deposits were observed on the right side of the city block but no longer existed in the site-city model, which is replaced with more stiff basement elements. On the other hand, the amplification of free-field site response caused by SCI is negligible and extends a short distance outside the city block.

City Response

The dynamic response of buildings is investigated in terms of the maximum roof drift ratio (RDR) under Models B and C with considering SCI. The RDR is calculated by dividing the maximum relative roof displacement (roof minus base) by the height of the building. The maximum RDR in the X-direction of a few buildings is summarized in Table 2. The buildings' numbers follow Figure 3(b).

Also, for all buildings except for Building 18, the maximum RDR of the idealized geometry of buildings produces similar or slightly smaller values than the actual geometry. However, the effect of building geometry in Building 18 is considerable, with the actual geometry producing 2.7 times the maximum RDR of the idealized geometry.

Table 2. Maximum RDR (%) in the X-direction of a few buildings in Models B and C

Building	Model B	Model C
1	0.07	0.08
2	0.07	0.07
9	0.06	0.07
10	0.16	0.16
12	0.05	0.07
18	0.07	0.18
20	0.04	0.05
22	0.04	0.05

CONCLUSIONS

This study introduces a site-city framework to model, analyze, and post-process seismic wave propagation in urban areas, accounting for site-city interaction. The framework includes novel features such as realistic terrain and surface topography modelling and the incorporation of subsurface geological and material heterogeneity. It also allows the generation of an unlimited number of buildings, accurately capturing their geometry, location, arrangement, and underground basement. The framework utilizes parallel computing on a supercomputer cluster to efficiently analyze and visualize results for large-scale site-city models.

A pilot study was conducted on a city block in downtown Toronto to showcase the capabilities of the developed site-city framework. In addition, a parametric study was conducted on three models, including the free-field site and idealized and actual geometry models of buildings in site-city models, to investigate the impact of SCI. The city block comprised 23 buildings, and the soil model was generated using 327 borehole logs to capture the geometric features and material heterogeneity with high accuracy.

The investigation focused on the structural response of buildings, particularly on the maximum roof drift ratio. The study analyzed two scenarios: one with actual building geometry and the other with idealized building geometry in site-city models. The results emphasized the significance of considering the actual geometry of buildings in assessing their structural response. The study found that the idealized geometry produced a slightly lesser response than the actual geometry. Also, modelling a building with high geometric irregularity, both in-plane and vertical, as a cuboid would significantly underestimate its dynamic response.

ACKNOWLEDGMENTS

The study is carried out with the support of Natural Sciences and Engineering Research Council of Canada (RGPIN-2021-03).

REFERENCES

[1] Gueguen, P., Bard, P.-Y., and Semblat, J. (2000). “From soil-structure to site-city interaction.” *Proceedings of the Twelfth World Conference on Earthquake Engineering*, Auckland, New Zealand.

[2] Fernandez-Ares, A. (2003). *Urban seismology: Interaction between earthquake ground motion and response of urban regions*. PhD Thesis, Department of Civil and Environmental Engineering, Carnegie Mellon University, Pittsburgh, Pennsylvania, USA.

[3] Bard, P.-Y., Gueguen, P., and Wirgin, A. (1996). “A note on the seismic wavefield radiated from large building structures into soft soils.” *Proceedings of the Eleventh World Conference on Earthquake Engineering*, Acapulco, Mexico.

[4] Chavez-Garcia, F. J., and Cardenas-Soto, M. (2002). “The contribution of the built environment to the ‘free-field’ ground motion in Mexico City.” *Soil Dynamics and Earthquake Engineering*, 22 (9-12), 773–780.

[5] Taborda, R. (2010). *Three dimensional nonlinear soil and site-city effects in urban regions*. PhD Thesis, Department of Civil and Environmental Engineering, Carnegie Mellon University, Pittsburgh, Pennsylvania, USA.

[6] Wong, H., and Trifunac, M. (1975). “Two-dimensional, antiplane, building-soil-building interaction for two or more buildings and for incident planet sh waves.” *Bulletin of the Seismological Society of America*, 65 (6), 1863–1885.

[7] Taborda, R., and Bielak, J. (2011). “Full 3D integration of site-city effects in regional scale earthquake simulations.” *Proceedings of Eighth International Conference on Structural Dynamics*, EURODYN, 511–518.

[8] Schwan, L., Boutin, C., Padron, L., Dietz, M. S., Bard, P.-Y., and Taylor, C. (2016). “Site-city interaction: Theoretical, numerical and experimental crossed-analysis.” *Geophysical Journal International*, 205 (2), 1006–1031.

[9] Isbiliroglu, Y., Taborda, R., and Bielak, J. (2015). “Coupled soil-structure interaction effects of building clusters during earthquakes.” *Earthquake Spectra*, 31 (1), 463–500.

[10] Sayed, M., Huang, X., and Kwon, O.-S. (2019). “A framework for multi-scale seismic simulation of a city block considering site–city interaction. ” *Proceedings of the Twelfth Canadian Conference on Earthquake Engineering*, Quebec City, Canada.

[11] Kato, B., and Wang, G. (2021). “Regional seismic responses of shallow basins incorporating site-city interaction analyses on high-rise building clusters.” *Earthquake Engineering & Structural Dynamics*, 50(1), 214–236.

[12] RockWorks17. (2019). Revision 2019.7.30 [software], Golden Co. USA: Rockware, Inc., https://www.rockware.com/product/rockworks/

[13] Hasancebi, N., and Ulusay, R. (2007). “Empirical correlations between shear wave velocity and penetration resistance for ground shaking assessments.” *Bulletin of Engineering Geology and the Environment*, 66, 203–213.

[14] Kato, B., and Wang, G. (2017). “Ground motion simulation in an urban environment considering site-city interaction: A case study of Kowloon Station, Hong Kong.” *Proceedings of the Third Huixian International Forum on Earthquake Engineering for Young Researchers*. University of Illinois Urbana-Champaign, Illinois, USA.

[15] Sayed, M. (2023). *Large-scale seismic soil-structure interaction simulation of civil infrastructures*. PhD Thesis, Department of Civil and Mineral Engineering, University of Toronto, Toronto, Ontario, Canada.

[16] Geuzaine, C., & Remacle, J.-F. (2009). Gmsh: A 3-d finite element mesh generator with builtin pre-and post-processing facilities. International Journal for Numerical Methods in Engineering, 79 (11), 1309–1331. https://gmsh.info/

[17] Systemes, D. (2013). Abaqus/standard user’s manual, version 6.13. https://www.3ds.com/products-services/simulia/products/abaqus/

[18] Utkarsh, A. (2015). The ParaView guide: A parallel visualization application. Kitware. Inc., New York. https://www.paraview.org/

[19] MATLAB. (2018). Version (r2018b). The MathWorks Inc, Natick, Massachusetts, USA. https://www.mathworks.com/products/matlab.html/

[20] Bavier, E., Hoemmen, M., Rajamanickam, S., and Thornquist, H. (2012). “Amesos2 and Belos: Direct and iterative solvers for large sparse linear systems.” *Scientific Programming*, 20(3), 241–255.

[21] Heroux, M., Bartlett, R., Howle, V., Hoekstra, R., Hu, J., Kolda, T., Lehoucq, R., Long, K., Pawlowski, R., Phipps, E., Salinger, A., Thornquist, H., Tuminaro, R., Willenbring, J., Williams, A., and Stanley, K. (2005). “An overview of the Trilinos project.” *ACM Transactions on Mathematical Software*, 31(3), 397–423.

[22] Ponce, M., van Zon, R., Northrup, S., Gruner, D., Chen, J., Ertinaz, F., Fedoseev, A., Groer, L., Mao, F., Mundim, B., Nolta, M., Pinto, J., Saldarriaga, M., Slavnic, V., Spence, E., Yu, C.-H., and Peltier, W. (2019). “Deploying a top-100 supercomputer for large parallel workloads: the Niagara supercomputer.” *Proceedings of the Practice and Experience in Advanced Research Computing* (PEARC), 1–8.